Optical Band Gap Modification of Single-Walled Carbon Nanotubes by Encapsulated Fullerenes

9 AUTHORS, INCLUDING:

Toshiya Okazaki
National Institute of Advanced Industrial Sci…
135 PUBLICATIONS **4,160** CITATIONS

SEE PROFILE

Soon-Kil Joung
FOOSUNG Co. Ltd
16 PUBLICATIONS **387** CITATIONS

SEE PROFILE

Minoru Otani
National Institute of Advanced Industrial Sci…
77 PUBLICATIONS **1,183** CITATIONS

SEE PROFILE

Susumu Okada
University of Tsukuba
220 PUBLICATIONS **3,251** CITATIONS

SEE PROFILE

Optical Band Gap Modification of Single-Walled Carbon Nanotubes by Encapsulated Fullerenes

Toshiya Okazaki,*,[†,‡] Shingo Okubo,[†] Takeshi Nakanishi,[†] Soon-Kil Joung,[†]
Takeshi Saito,[†,‡] Minoru Otani,[§] Susumu Okada,[⊥] Shunji Bandow,[‖] and
Sumio Iijima[†,‖]

*Research Center for Advanced Carbon Materials, National Institute of Advanced Industrial
Science and Technology (AIST), Tsukuba 305-8565, Japan, PRESTO, Japan Science and
Technology Agency (JST), 4-1-8 Honcho, Kawaguchi 332-0012, Japan, Institute for Solid State
Physics, University of Tokyo, 5-1-5 Kashiwanoha, Kashiwa 277-8581, Japan, Institute of Physics
and Center for Computational Sciences, University of Tsukuba, 1-1-1 Tennodai, Tsukuba
305-8577, Japan, CREST, Japan Science and Technology Agency, 4-1-8 Honcho, Kawaguchi
332-0012, Japan, and Department of Materials Science and Engineering,
Meijo University, 1-501 Shiogamaguchi, Tempaku-ku, Nagoya 468-8502, Japan*

Received December 14, 2007; E-mail: toshi.okazaki@aist.go.jp

Abstract: We report optical band gap modifications of single-walled carbon nanotubes upon C_{60} insertions by using photoluminescence and the corresponding excitation spectroscopy. The shifts in optical transition energies strongly depend on the tube diameter (d_t) and the "$2n + m$" family type, which can be explained by the local strain and the hybridization between the nanotube states and the C_{60} molecular orbitals. The present results provide possible design rules for nanotube-based heterostructures having a specific type of electronic functionality.

Introduction

Today, the physical and economic limitations of conventional top-down technologies are widely recognized, and alternative bottom-up techniques are being considered.[1] In these techniques, individual molecules can perform functions identical or analogous to those of transistors, diodes, conductors, and other key components of microcircuits.[1] Single-walled carbon nanotubes (SWNTs) have been expected as building blocks for such molecular electronics because of their unique electronic and mechanical properties.[2] Advantageously, the local electronic band gap of SWNTs can be tuned by incorporating fullerene molecules, which results in nanometer-scale structured materials containing multiple quantum dots with lengths of ∼10 nm.[3,4] For example, low-temperature scanning tunneling spectroscopy (LT-STS) revealed that a band gap of ∼0.5 eV is narrowed down to ∼0.1 eV at the site where a $Gd@C_{82}$ molecule is inserted in semiconducting (11, 9) SWNT material.[3] Although it provides possible design rules for proposing hybrid structures having a specific type of electronic functionality, the effect of encapsulated fullerene molecules on the band gap modifications of SWNTs is yet unclear from either the experimental or theoretical points of view.

On the other hand, the recent discovery of band gap photoluminescence (PL) of SWNTs has paved the way for investigating their unique electronic properties induced by low dimensionality.[5] The origin of the observed PL peak was reliably assigned to SWNTs with specific chiral indexes (n, m) because the emission and excitation spectra show characteristic peaks depending on the molecular structure of SWNTs. Consequently, the PL method can provide rich information about electronic properties for individual (n, m) nanotubes at a resolution of a few milli-electron volts. We report here systematic studies on the optical band gap modification of C_{60} encapsulating SWNTs, so-called nanopeapods, by using a two-dimensional (2D) PL excitation/emission mapping method. It is found that differences in the optical transition energies between unfilled semiconducting SWNTs and the corresponding C_{60} nanopeapods strongly depend on the tube diameter and "$2n + m$" family types (type I ($\mathrm{mod}(2n + m, 3) = 1$) and type II ($\mathrm{mod}(2n + m, 3) = 2$)). The change in optical band gap is rationally explained by the local strain of SWNTs upon C_{60} insertion and hybridization of the electronic states between the encapsulated C_{60} and the outer SWNTs.

Experimental Section

We used two kinds of SWNTs that were produced by the pulsed laser vaporization (PLV) method[6] and the direct-injection-pyrolutic-synthesis (DIPS) method.[7] The details of the purification procedure for the PLV-SWNTs were reported previously.[6] The SWNTs were

† AIST.
‡ PRESTO.
§ University of Tokyo.
⊥ University of Tsukuba and CREST.
‖ Meijo University.
(1) The International Technology Roadmap for Semiconductors (ITRS): Emerging Research Devices. http://www.itrs.net/reports.html.
(2) Avouris, P.; Chen, J. *Mater. Today*, **2006**, *9*, 46−54.
(3) Lee, J.; Kim, H.; Kahng, S.-J.; Kim, G.; Son, Y.-W.; Ihm, J.; Kato, H.; Wang, Z. W.; Okazaki, T.; Shinohara, H.; Kuk, Y. *Nature*, **2002**, *415*, 1005−1008.
(4) Hornbaker, D. J.; Kahng, S.-J.; Misra, S.; Smith, B. W.; Johnson, A. T.; Mele, E. J.; Luzzi, D. E.; Yazdani, A. *Science*, **2002**, *295*, 828−831.
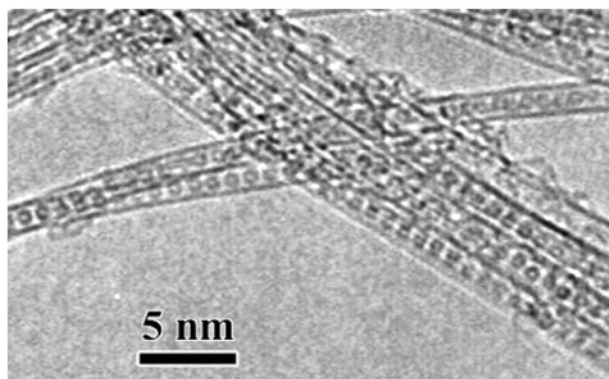
Figure 1. Typical HRTEM image of C_{60} nanopeapods.

heated in dry air at ~500 °C for 30 min to open the tube ends. The encapsulation of C_{60} into the open-ended SWNTs was achieved through gas-phase reaction.[6] Transmission electron microscope (TEM) images were taken with a JEOL 2010F microscope operated at 120 kV. Aqueous micellar solutions of C_{60} nanopeapods for PL measurements were prepared in a procedure similar to the procedure described by Bachilo et al.[8] We used dodecylbenzene sulfonate (SDBS) and sodium cholate (SC) as surfactants. The PL mapping was performed with a Shimadzu NIR-PL system utilizing an IR-enhanced InGaAs detector (Princeton instruments OMA-V2.2) for detection and a tunable Ti-sapphire laser (Spectra Physics 3900S) for excitation. The slit width for emission was 10 nm. Typical scan steps were 5 and 2 nm for excitation and emission, respectively. The raw data were corrected for wavelength-dependent instrumental factors and excitation laser intensities. Optical absorption spectra were recorded with a Shimadzu UV-3150 spectrometer. Resonant Raman spectra were measured with a triple-grating monochromator (Bunko-Keiki BRM-900) equipped with an InGaAs diode array using a tunable Ti-sapphire laser (Spectra Physics 3900S) for excitation. Details of theoretical calculations were described previously.[9] Briefly, the electronic-structure calculation and the geometry optimizations were performed using the local-density approximation in the density function theory with the plane wave basis set and the norm-conserving pseudo-potential.

Results and Discussion

TEM Observations. Figure 1 shows a typical high-resolution transmission electron microscope (HRTEM) image of the synthesized C_{60} nanopeapods. The HRTEM image clearly shows that the C_{60} units are closely packed inside the SWNTs.

Photoluminescence (PL) Spectra. Figure 2A shows a 2D PL contour plot of the unfilled PLV-SWNTs in SDBS−D_2O as a function of emission (λ_{11}) and excitation (λ_{22}) wavelengths. The PL maxima (spots) on the map are clearly seen in the second interband (E_{22}) excitation region ($\lambda_{22} = 800-1000$ nm) and the first interbands (E_{11}) emission region ($\lambda_{11} = 1400-1700$ nm) of SWNTs with 1.2−1.4 nm in diameter, which can be assigned to the specific (n, m) SWNTs by using the empirical relations of Weisman et al.[10] It is noted that all peak positions were slightly and uniformly red-shifted after the tube opening (~5

meV in E_{11} and ~8 meV in E_{22}). This can be explained by the presence of the solvents in the interior space of the open-ended SWNTs. Actually, it has been known that water molecules are encapsulated inside SWNTs.[11] The filling water solvents should cause a reduction of the electron−electron repulsion and the exciton binding energy by dielectric screen effects,[12] which results in the observed red shifts.

Overall features of the PL behavior of SWNTs drastically change upon fullerene encapsulations. Figure 2B shows the 2D PL contour map of C_{60} nanopeapods in SDBS−D_2O. Obviously, the PL peaks in Figure 2B can be divided into two groups (the white line in Figure 2B). One is the peaks whose positions are the same as those of unfilled SWNTs. The origins of these peaks are thus easily assigned to the (11, 6), (15, 1), (10, 8), (12, 5), and (11, 7) tubes, respectively (Figure 2B). The characteristic feature of this group is that the tube diameters are less than ~1.25 nm. On the other hand, the original PL peaks of larger diameter tubes with $d_t > 1.25$ nm such as (13, 5), (12, 7), and (10, 9) tubes almost completely disappear in Figure 2B. Alternatively, new PL peaks appear at positions different from those of the unfilled SWNTs. The threshold diameter of ~1.25 nm closely matches the theoretically predicted value of ~1.28 nm for unstrained filling of C_{60}.[13] This agreement strongly suggests that C_{60} is preferentially encapsulated into SWNTs with $d_t > 1.25$ nm and that the filling causes spectral shifts for those nanotubes. The strongest PL peaks of the (13, 5) tube in Figure 2A presumably move to the new strongest PL peak in Figure 2B because the filling can be assumed to not significantly affect the quantum efficiency.[14,15] Likewise, the second and third strongest peaks in Figure 1B can be assigned to the (12, 7) and (10, 9) tubes, respectively. The arrows in Figure 2B indicate the shifts of the PL peak positions of these SWNTs.

To unambiguously assign the new peaks to specific (n, m) tubes, we further examined another sample that has a different chirality distribution and a different filling yield. Parts C and D of Figure 2 present the PL contour plot for PLV-SWNTs and the corresponding C_{60} nanopeapods with a lower filling yield. Some peaks can be attributed to the unfilled tubes, while there are other peaks which are shifted due to C_{60} encapsulations. The observation of the process of the shifts in the partially filled sample, for example, the (12, 7), (16, 2), and (13, 6) tubes, is a confirmation of the observed shifts for both excitation and emission. An important difference between the PL maps in parts B and D of Figure 2 is that the PL peaks at (λ_{11}, λ_{22}) = (1382 nm, 1015 nm) and (1776 nm, 816 nm) cannot be seen in Figure 2D. Because the diameters of the (14, 3) and (15, 2) tubes are just on the smallest limit of C_{60} encapsulation, the filling yields of these tubes are much lower than the others and the corresponding PL peaks are missing. Hence, the PL peaks at (λ_{11}, λ_{22}) = (1382 nm, 1015 nm) and (1776 nm, 816 nm) can be assigned to the (14, 3) and (15, 2) tubes, respectively. This peak assignment of the (14, 3) tube was verified by the resonance Raman spectroscopy (see below).

(5) Weisman, R. B. In *Applied Physics of Carbon Nanotubes: Fundamentals of Theory, Optics and Transport Devices*; Rotkin, S. V., Subramoney, S., Eds.; Springer: Berlin, 2005; pp 183−202.
(6) Hirahara, K.; Suenaga, K.; Bandow, S.; Kato, H.; Okazaki, T.; Shinohara, H.; Iijima, S. *Phys. Rev. Lett.*, **2000**, *85*, 5384−5386.
(7) Saito, T.; Ohshima, S.; Xu, W.-C.; Ago, H.; Yumura, M.; Iijima, S. *J. Phys. Chem. B* **2005**, *109*, 10647−10652.
(8) Bachilo, S. M.; Strano, M. S.; Kittrell, C.; Hauge, R. H.; Smalley, R. E.; Weisman, R. B. *Science* **2002**, *298*, 2361−2366.
(9) Otani, M.; Okada, S.; Oshiyama, A. *Phys. Rev. B: Condens. Matter Mater. Phys.* **2003**, *68*, 125424.
(10) Weisman, R. B.; Bachilo, S. M. *Nano Lett.* **2003**, *3*, 1235−1238.

(11) Maniwa, Y.; Kataura, H.; Abe, M.; Suzuki, S.; Achiba, Y.; Kira, H.; Matsuda, K. *J. Phys. Soc. Jpn.* **2002**, *71*, 2863−2866.
(12) Ando, T. *J. Phys. Soc. Jpn.* **2004**, *73*, 3351−3363.
(13) Okada, S.; Saito, S.; Oshiyama, A. *Phys. Rev. Lett.* **2001**, *86*, 3835−3838.
(14) Li, L.-J.; Khlobystov, A. N.; Wiltshire, J. G.; Briggs, G. A. D.; Nicholas, R. J. *Nat. Mater.* **2005**, *4*, 481−485.
(15) Li, L.-J.; Lin, T.-W.; Doig, J.; Mortimer, I. B.; Wiltshire, J. G.; Taylor, R. A.; Sloan, J.; Green, M. L. H.; Nicholas, R. J. *Phys. Rev. B: Condens. Matter Mater. Phys.* **2006**, *74*, 245418.
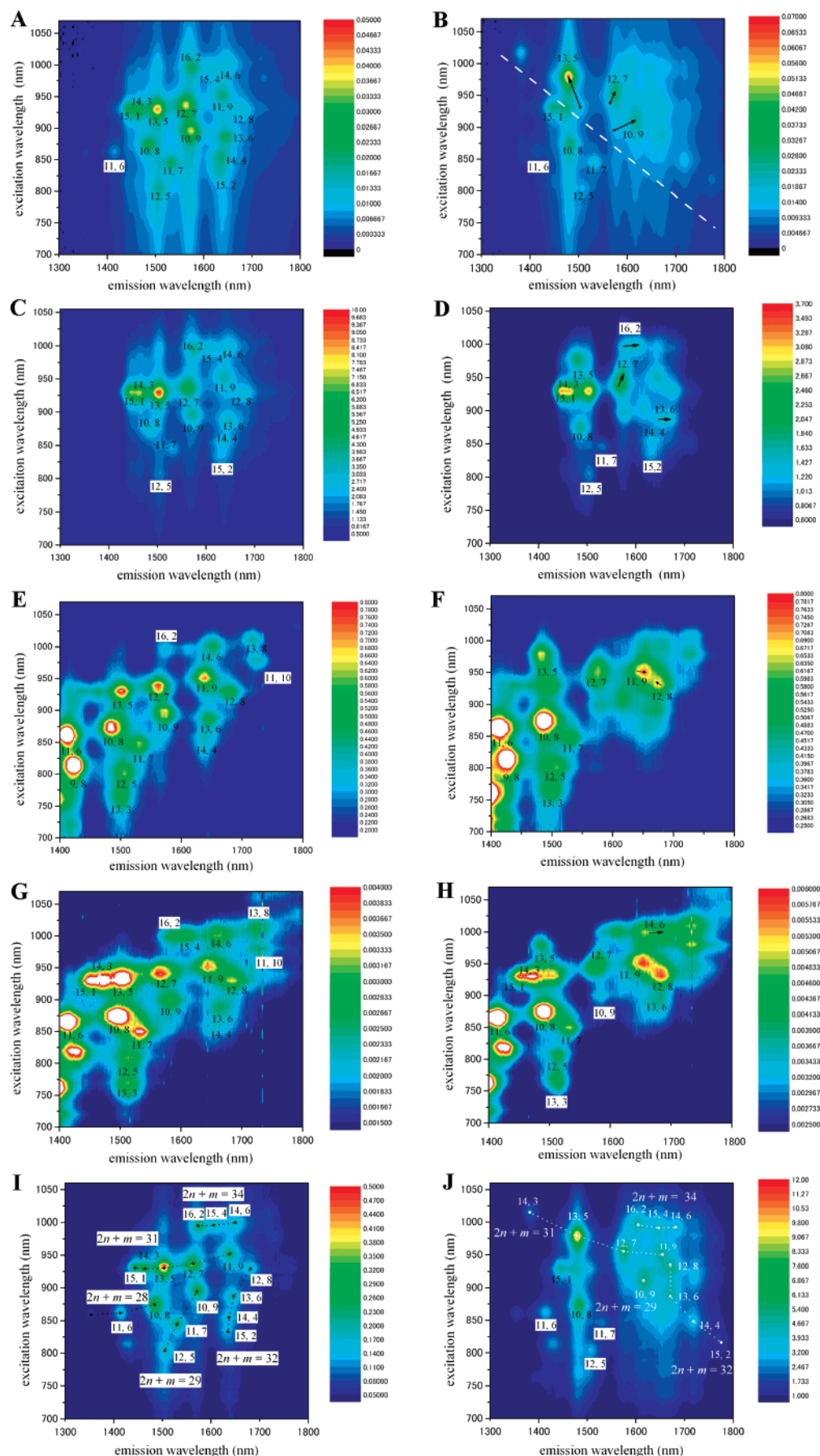
Figure 2. 2D PL contour plots of (A, C, E, G, I) SWNTs and (B, D, F, H, J) the corresponding C_{60} nanopeapods in (A, B, C, D, E, F, I, J) SDBS−D_2O and (G, H) SC−D_2O solutions.

Table 1. Optical Transition Energies of SWNTs and C_{60} Nanopeapods in SDBS−D_2O and the Energy Differences between Them ($\Delta E_{ii} = E_{ii}{}^{nanopeapods} - E_{ii}{}^{SWNTs}$, $i = 1, 2$)
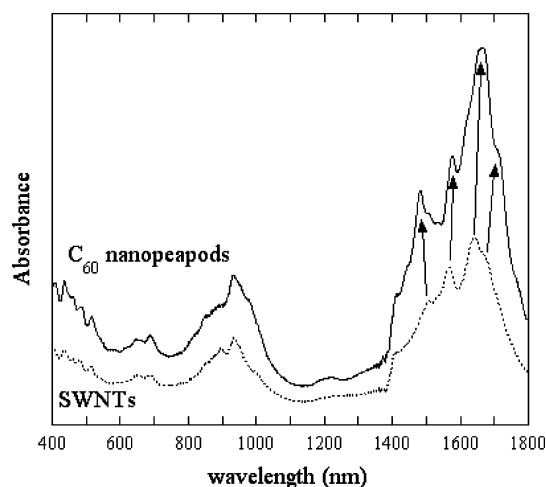
	SWNTs		C_{60} nanopeapods			
	E_{11}	E_{22}	E_{11}	E_{22}	ΔE_{11}	ΔE_{22}
(n, m)	(eV)	(eV)	(eV)	(eV)	(meV)	(meV)
			Type I			
(14, 3)	0.847	1.335	0.897	1.221	50	−114
(13, 5)	0.826	1.334	0.838	1.268	12	−66
(12, 7)	0.794	1.324	0.788	1.299	−6	−25
(16, 2)	0.788	1.245	0.772	1.243	−16	−2
(11, 9)	0.757	1.303	0.751	1.305	−6	2
(15, 4)	0.771	1.242	0.752	1.249	−19	7
(14, 6)	0.752	1.236	0.736	1.249	−16	13
			Type II			
(15, 2)	0.758	1.488	0.698	1.520	−60	32
(14, 4)	0.758	1.450	0.722	1.460	−36	10
(10, 9)	0.789	1.386	0.767	1.361	−22	−25
(13, 6)	0.753	1.398	0.743	1.395	−10	-3
(12, 8)	0.738	1.335	0.742	1.328	4	−7

Figure 3. UV−vis−NIR absorption spectra of C_{60} nanopeapods−SDBS−D_2O and SWNT−SDBS−D_2O solutions.

Parts E and F of Figure 2 show the 2D PL contour plots of DIPS-SWNTs and the corresponding C_{60} nanopeapods, respectively. Because the PL intensities of the (11, 9) and (12, 8) tubes are prominent in the longer wavelength region ($\lambda_{11} > 1600$ nm and $\lambda_{22} > 900$ nm), the PL peaks of the (11, 9) and (12, 8) tubes after C_{60} insertions are easily assigned, as shown in Figure 2F.

The other example of the PL contour plots of SWNTs and the corresponding nanopeapods are shown in parts G and H of Figure 2 respectively, where DIPS-SWNTs and SC were used as templates for nanopeapods and a surfactant. Even for a different surfactant, characteristic features of the spectral shifts remain unchanged, indicating that the observed energy shifts are unlikely to result from the specific interaction between the nanopeapods and the surfactants. The filling yield of this sample is also lower than that of the samples shown in part B of Figure 2 (and part F), which results in the clear spectral shift upon C_{60} encapsulation. Especially, the direction of the shift is clearly seen in the (14, 6) tubes.

The origins of the remaining new PL peaks at $(\lambda_{11}, \lambda_{22}) = $ (1655 nm, 994 nm) and (1719 nm, 848 nm) (see Figure 2B) can be identified by considering the family pattern of SWNTs.[5] Figure 2I shows the PL contour plot of PLV-SWNTs in which the PL peaks with the same $2n + m$ values are connected. This $2n + m$ family pattern is same as the previously reported data.[5] On the other hand, Figure 2J shows the 2D PL contour plot of C_{60} nanopeapods. According to the above discussion, new PL peaks of the (10, 9), (14, 3), (13, 5), (12, 7), (11, 9), (15, 2), (13, 6), (12, 8), (16, 2), and (14, 6) tubes can be assigned (solid circles). The remaining PL peaks at $(\lambda_{11}, \lambda_{22}) = $ (1655 nm, 994 nm) and (1719 nm, 848 nm) locate between those of (16, 2) and (14, 6) tubes and (13, 6) and (15, 2) tubes, respectively. Therefore, they are reasonably attributed to the (15, 4) and (14, 4) tubes, respectively. The obtained PL peak positions of SWNTs and C_{60} nanopeapods in SDBS−D_2O solutions are summarized in Table 1.

Optical Absorption Spectra. Figure 3 presents an UV−vis−NIR absorption spectrum of C_{60} nanopeapods in SDBS micellar solution, together with the reference spectrum of the unfilled SWNTs. The spectral changes upon C_{60} encapsulation are clearly observed in the first interband (E_{11}) region ($\lambda_{11} = 1400-1700$ nm). For instance, the absorption peak at ∼1500 nm in SWNTs

is blue-shifted to ∼1480 nm, which is almost identical to the change in the emission wavelength of the (13,5) tubes (Figure 2B). On the other hand, absorption peaks at ∼1570, ∼1640, and ∼1670 nm in SWNTs are red-shifted to ∼1580, 1670, and ∼1720 nm, respectively, upon C_{60} insertions, which is consistent with the changes in the PL emission wavelengths with $\lambda_{11} > $ ∼1550 nm (Figure 2B,D,F). In particular, the absorption at ∼1720 nm in C_{60} nanopeapods can be attributed to the (14, 4) tubes (Figure 2I,J).

It is well-known that charge transfer between the encapsulated molecules and the host SWNTs decreases the E_{11} absorption band.[16] The lack of severe decrease of absorption intensity indicates an absence of charge transfer between C_{60} and the host SWNTs.

Resonance Raman Spectra. Figure 4A shows the resonant Raman spectra of C_{60} nanopeapods and SWNTs in SDBS micellar solutions under 1000 nm excitation. For unfilled SWNTs, a strong radial breathing mode (RBM) was observed at 182 cm^{-1}, which corresponds to SWNTs with d_t ∼1.3 nm. In addition to this, a new RBM appears at 197 cm^{-1} for C_{60} nanopeapods, which can be attributed to smaller diameter tubes (d_t ∼1.2 nm). An appearance of the RBM of smaller diameter tubes under 1000 nm excitation strongly suggests that the origin of the PL peak at $\lambda_{22} = 1015$ nm excitation (Figure 2B,J) is the (14, 3) tubes (d_t ∼1.248 nm[10]). As a result of the strong modification in E_{22} upon C_{60} encapsulation, (14, 3) tubes move into resonance (Figure 2B,J).

The RBM frequency is also affected by fullerene encapsulation. In fact, the observed value of 197 cm^{-1} is slightly larger than that of the unfilled (14, 3) tube (191.6 cm^{-1}).[10] Recently, Okada reported that the RBM frequencies of smaller diameter SWNTs (d_t < ∼1.4 nm) shift upward by C_{60} encapsulations.[17] For (9, 9) and (10, 10) tubes (d_t = 1.22 and 1.37 nm, respectively), 86 and 3 cm^{-1} upshifts were predicted by the theoretical calculations.[17] The observed upshift of ∼5 cm^{-1} for (14, 3) tube (Figure 4A) is a reasonable value because the diameter of the (14, 3) tube is between those of the (9, 9) and (10, 10) tubes. Such high-frequency shifts by the fullerene encapsulations were also reported by Bandow et al.[18] The upshift

(16) Kavan, L.; Rapta, P.; Dunsch, L.; Bronikowski, M. J.; Willis, P.; Smalley, R. E. *J. Phys. Chem. B* **2001**, *105*, 10764−10771.
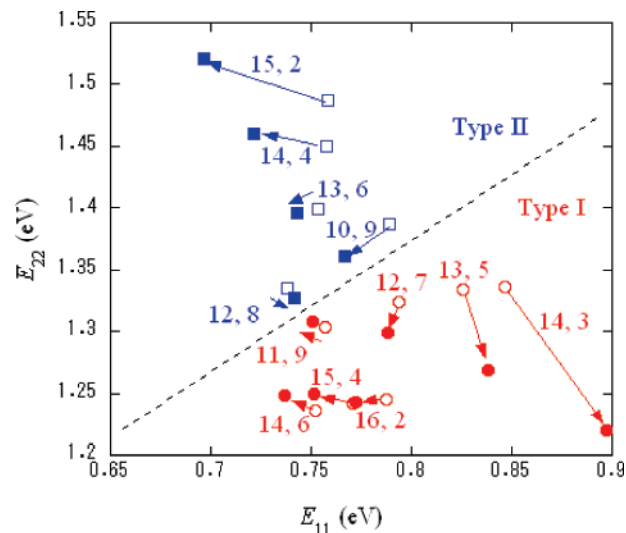(17) Okada, S. *Chem. Phys. Lett.* **2007**, *438*, 59−62.
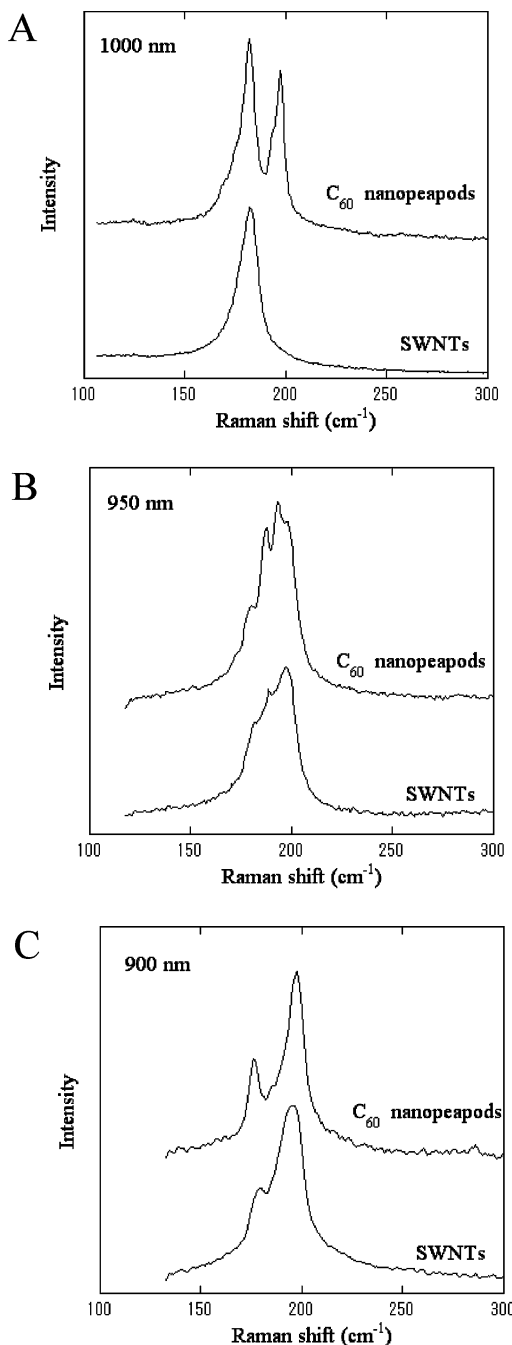
Figure 4. Resonance Raman spectra of C_{60} nanopeapods−SDBS−D_2O and SWNT−SDBS−D_2O solutions. Excitation wavelengths for the resonant Raman spectra are (A) 1000 nm, (B) 950 nm, and (C) 900 nm.

Figure 5. The shifts in optical transition energies (E_{11} and E_{22}) of SWNTs upon C_{60} encapsulations in SDBS micellar solutions.

of ~2 cm^{-1} was experimentally observed for SWNTs with d_t ~1.37 nm upon C_{60} encapsulations.

In contrast, such a drastic change in the line shape of RBM was not observed at lower excitation wavelengths because energy differences in E_{22} between SWNTs and C_{60} nanopeapods are much smaller for other tubes than that of (14, 3) tubes (Figure 2). Indeed, the obtained RBM of C_{60} nanopeapods shows a spectral shape similar to those of unfilled SWNTs under the 950 and 900 nm excitations (Figure 4B,C).

Mechanisms for the Optical Band Gap Modification. Returning to the PL spectral shifts upon C_{60} encapsulations,

Figure 5 shows the corresponding energy shifts in E_{11} and E_{22} for each (n, m) nanotube, where the open circles and squares represent unfilled SWNTs and the filled circles and squares represent C_{60} nanopeapods (Table 1). The broken line indicates a boundary between type I and type II SWNTs. Interestingly, the changes in the optical transition energies strongly depend on the $2n + m$ family type. A symmetric pattern about the broken line is clearly seen in Figure 5.

In order to investigate the modification mechanism in detail, the energy differences in E_{11} and E_{22} between C_{60} nanopeapods and SWNTs ($\Delta E_{ii} \equiv E_{ii}^{nanopeapods} - E_{ii}^{SWNTs}$, $i = 1, 2$) are plotted as a function of tube diameter and a chiral angle (θ) (Figure 6). The diameter dependencies of ΔE_{11} and ΔE_{22} are different between type I and type II tubes. With increasing tube diameter, ΔE_{11} values for type I tubes exponentially decrease toward −0.02 eV, while ΔE_{11} values for type II tubes increase (Figure 6A). On the other hand, ΔE_{22} values for type I tubes increase with increasing tube diameter, whereas ΔE_{22} values for type II tubes exhibit an opposite trend (Figure 6B).

Such strong dependences on $2n + m$ family type and tube diameter in ΔE_{11} and ΔE_{22} remind us of strain-induced spectral shift.[19] For instance, theoretical simulations predicted that the band gap of (17, 0) tubes (type I) increases by ~0.1 eV upon C_{82} fullerene insertion, which is dominated by the local radial strain.[20,21] A similar situation should occur in $(C_{60})_n@(14, 3)$ nanopeapods (type I) because the spacing between the (17, 0) tube and the C_{82} unit is almost identical to that in $(C_{60})_n@(14, 3)$ (=0.26−0.27 nm). Indeed, the calculated energy shifts of ~0.1 eV[20,21] in E_{11} and from −0.21 to −0.26 eV[21] in E_{22} for $(C_{82})_n@(17, 0)$ are very similar to $\Delta E_{11} = 0.050$ eV and $\Delta E_{22} = -0.116$ eV for $(C_{60})_n@(14, 3)$. Furthermore, the zigzag tubes ($\theta = 0°$) are more sensitive to such strains than the arm-chair tubes ($\theta = 30°$),[19] which agrees with the observed trend in Figure 3C,D. Moreover, the effective-mass theory predicts that the strain-induced change in E_{11} shows opposite sign to that in

(18) Bandow, S.; Takizawa, M.; Kato, H.; Okazaki, T.; Shinohara, H.; Iijima, S. *Chem. Phys. Lett.* **2001**, *347*, 23−28.

(19) Yang, L.; Han, J. *Phys. Rev. Lett.* **2000**, *85*, 154−157.
(20) Cho, Y.; Han, S.; Kim, G.; Lee, H.; Ihm, J. *Phys. Rev. Lett.* **2003**, *90*, 106402.
(21) Lu, J.; Nagase, S.; Re, S.; Zhang, X.; Yu, D.; Zhang, J.; Han, R.; Gao, Z.; Ye, H.; Zhang, S.; Peng, L. *Phys. Rev. B: Condens. Matter Mater. Phys.* **2005**, *71*, 235417.
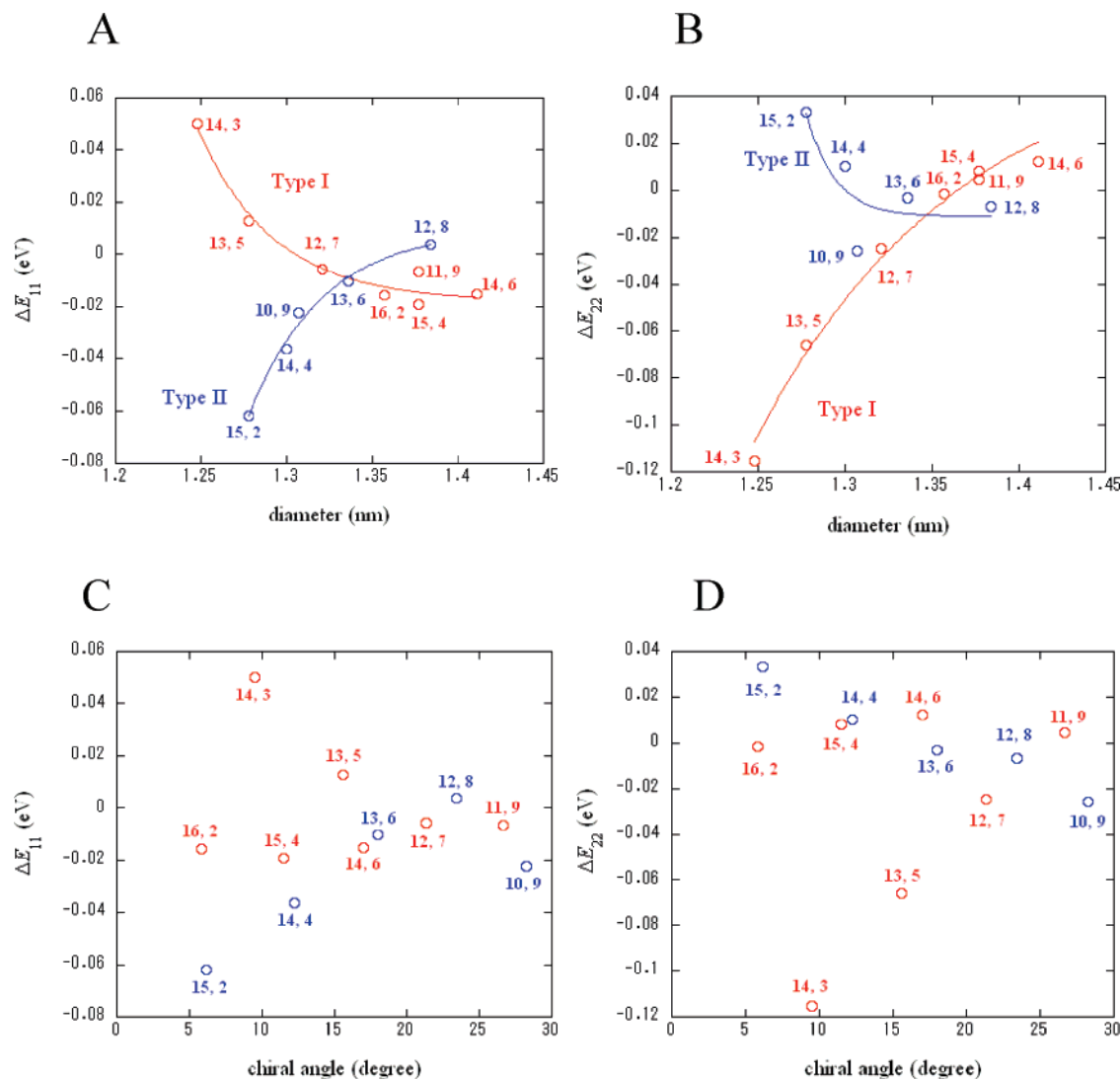
Figure 6. Differences in optical transition energies in E_{11} and E_{22} (ΔE_{11} and ΔE_{22}, respectively) between C_{60} nanopeapods and SWNTs as a function of (A and B) tube diameter and (C and D) chiral angle.

E_{22} within a noninteracting model.[22] This characteristic feature can clearly be seen in SWNTs with $d_t < \sim 1.3$ nm (Figure 6A,B and Table 1). These results strongly suggest that the energy shifts of smaller diameter tubes such as (14, 3), (13, 5), and (15, 2) are induced by strain effects.
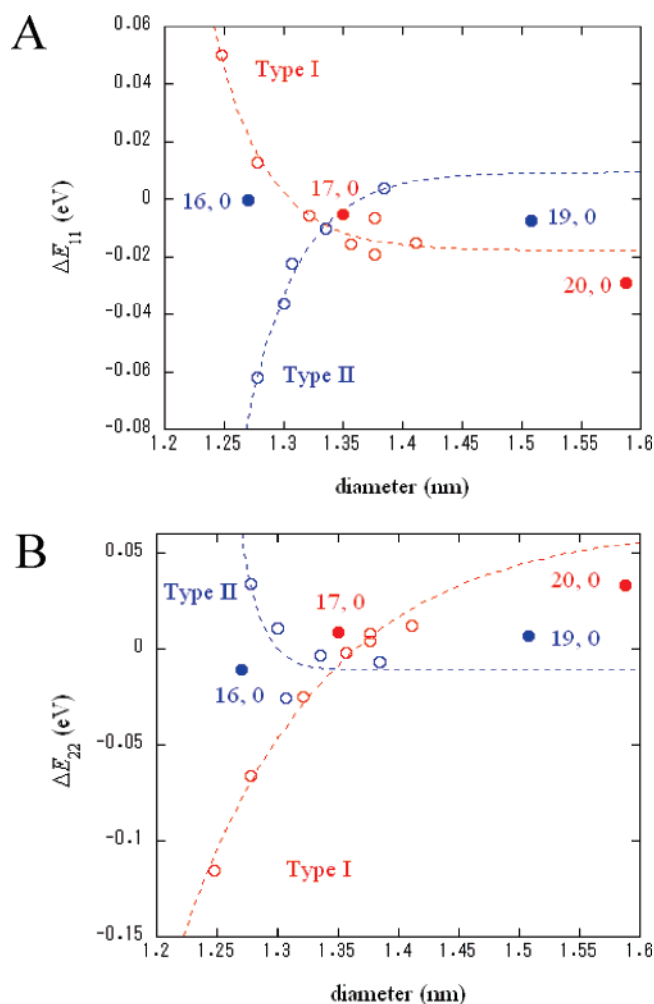
The insertion of an oversized fullerene may cause a radial expansion around fullerene and a local compressive stress along the tube axis.[20] The energy gap change (ΔE_{gap}) between the first van Hove singularities under the uniaxial stress can be expressed as

$$\Delta E_{\text{gap}} = -\text{sgn}(2p + 1)3t_0(1 + \nu)\sigma \cos 3\theta \qquad (1)$$

where $p = \text{mod}(n - m, 3)$, t_0 is the hopping parameter, ν is Poisson's ratio, and σ is the radial expansion and/or the tube compression, respectively.[19,21] Taking $t_0 = 2.66$ eV and $\nu = 0.2$,[19] we obtain $\sigma = 0.6\%$ for reproducing the observed ΔE_{11} value of (14, 3) nanopeapods (=0.050 eV) with eq 1. Such a small strain is sufficient for explanation of the obtained band gap shift.

(22) Suzuura, H.; Ando, T. *Phys. Rev. B: Condens. Matter Mater. Phys.* **2002**, *65*, 235412.

With increasing tube diameter, the local strain upon C_{60} encapsulation should disappear and ΔE_{11} and ΔE_{22} should approach zero. Theoretical calculations predict that structural deformation does not occur at $d_t > \sim 1.3$ nm.[9,13] However, we observed nonzero values of ΔE_{11} and ΔE_{22} even for the larger diameter tubes (Figure 6A,B). In such a larger diameter regime, the band gap shifts can be explained by the hybridization between the π states of C_{60} and the nearly free electron (NFE) states of SWNTs.[13] In Figure 7, the calculated ΔE_{11} and ΔE_{22} values for several zigzag $(n, 0)$ nanotubes encapsulating C_{60} are presented as a function of tube diameter,[9] together with the experimental data. The calculated energy shifts can be attributed to a coupling between the t_{1u} state of C_{60} and the NFE states.[9] It is clear that the family type and the tube diameter dependences are quasi-quantitatively reproduced by the calculations. Even though the calculated ΔE_{11} and ΔE_{22} values reproduce well the experimental observations in $d_t > 1.3$ nm, a significant discrepancy remains in the (16, 0) tubes. This discrepancy indicates that the local strain effect might be underestimated in the theoretical calculations. The remaining question is to be solved in future calculations with chiral nanotubes.

Figure 7. Calculated ΔE_{11} and ΔE_{22} values in zigzag C_{60} nanopeapods (solid circles) as a function of a tube diameter, together with those obtained by the PL experiments (open circles).

It has been established that the PL behaviors of SWNTs are dominated by the Coulomb interaction between the optically produced electron−hole pairs (exitons).[23] Upon the fullerene insertions, exciton effects such as electron−electron repulsion and electron−hole attraction should be screened.[12] Even though the screen effect affect the optical band gap, it is un-likely that it depends on the $2n + m$ family type.[12] Furthermore, the observed ΔE_{11} and ΔE_{22} values are semiquantitatively reproduced by theoretical calculations in which hybridization between the C_{60} orbitals and the nanotube states undergoes energy shifts (Figure 7). Therefore, the exciton effects are excluded as a primary reason for the observed band gap modifications.

Conclusion

In summary, optical band gap modifications of SWNTs upon fullerene insertion were successfully observed by the 2D PL method. The obtained energy shifts were understandable in terms of the local strain effects of SWNTs and hybridization of the energy levels between encapsulated fullerenes and outer SWNTs. Interestingly, a decrease of 36 meV in E_{11} for C_{60}@(14, 4) nanopeapods having $d_t = 1.30$ nm is in remarkable agreement with a previous LT-STS study in which a down shift in the first van Hove band gap of $\sim$60 meV was observed for SWNTs with $d_t \sim 1.3$ nm upon C_{60} encapsulation.[4] This suggests that the present findings provide general rules for the band gap engineering of SWNTs, which could result in one-dimensional nanotube devices having multiple quantum dots.

(23) Wang, F.; Dukovic, G.; Brus, L. E.; Heinz, T. F. *Science*, **2005**, *308*, 838−841.